

# A 15-Year Climatology of Desert Dust Episodes in the Broader Mediterranean Basin <sup>†</sup>

Maria Gavrouzou <sup>1,\*</sup>, Nikos Hatzianastassiou <sup>1</sup>, Antonis Gkikas <sup>2</sup> and Nikos Mihalopoulos <sup>3,4</sup>

<sup>1</sup> Laboratory of Meteorology and Climatology, Department of Physics, University of Ioannina, 451 10 Ioannina, Greece; nhatzian@uoi.gr

<sup>2</sup> Institute for Astronomy, Astrophysics Space Applications and Remote Sensing, National Observatory of Athens, 152 36 Athens, Greece; agkikas@noa.gr

<sup>3</sup> Institute for Environmental Research and Sustainable Development (IERSD), NOA, 152 36 Athens, Greece; mihalo@uoc.gr

<sup>4</sup> Environmental Chemical Processes Laboratory, Department of Chemistry, University of Crete, 700 13 Heraklion, Greece

\* Correspondence: gavrouzou.m@gmail.com

<sup>†</sup> Presented at the 3rd International Electronic Conference on Atmospheric Sciences, 16–30 November 2020; Available online: <https://ecas2020.sciforum.net/>.

**Abstract:** In the present study, dust aerosol episodes (DAEs) in the broader Mediterranean Basin (MB) are investigated over a 15-year (2005–2019) period using contemporary MODIS Collection 6.1 and OMI OMAERUV satellite data and a satellite algorithm applying a thresholding technique on selected aerosol optical properties. The algorithm operates on a daily and  $1^\circ \times 1^\circ$  pixel level basis, first identifying the presence of dust, and consequently requiring the presence of unusually high dust loads, i.e., dust episodes. Apart from the presence of pixel-level DAEs, an extended spatial coverage of dust is also required. Thus, a specific day is characterized as a Dust Aerosol Episode Day (DAED), when at least 30 episodic pixels exist over Mediterranean Basin (MB). According to the algorithm results, 166 DAEDs (116 strong and 50 extreme) took place in the MB from 2005 to 2019. Most DAEDs occurred in spring (47%) and summer (38%), while a different seasonality is observed for strong and extreme episodes. The interannual variability of DAEDs reveal a decreasing trend, which is however not statistically significant.

**Keywords:** dust episodes; Mediterranean; satellite data; climatology

**Citation:** Gavrouzou, M.; Hatzianastassiou, N.; Gkikas, A.; Mihalopoulos, N. A 15-Year Climatology of Desert Dust Episodes in the Broader Mediterranean Basin. *Environ. Sci. Proc.* **2021**, *4*, 1. <https://doi.org/10.3390/ecas2020-08138>

Academic Editor: Anthony R. Lupu

Published: 13 November 2020

**Publisher's Note:** MDPI stays neutral with regard to jurisdictional claims in published maps and institutional affiliations.



**Copyright:** © 2020 by the authors. Licensee MDPI, Basel, Switzerland. This article is an open access article distributed under the terms and conditions of the Creative Commons Attribution (CC BY) license (<http://creativecommons.org/licenses/by/4.0/>).

## 1. Introduction

Dust is the Earth's most abundant aerosol type, mostly originating from great deserts (Sahara, Taklimakan, Gobi, Middle East), but also from agricultural and construction activities. The emitted dust remains in the atmosphere from a few hours up to several days, while under favorable conditions it is transported far from its sources. During this transport, the physical and chemical properties of dust can change, thus affecting its action as Cloud Condensation Nuclei (CCN) or Ice Nuclei (IN) as well as its interaction with radiation. Given that it acts as CCN and/or IN, dust modifies the physical and optical properties of clouds and consequently their lifetime and precipitation efficiency. It has been found that aerosols, including dust, increase the Cloud Droplet Number Concentration (CDNC) while decreasing the cloud effective radius, thus leading to reduced precipitation and cloud dissipation [1]. However, Aerosol Cloud Interactions (ACI) vary depending not only on the aerosol type, but also on the cloud type. Thus, it was found [2] that ACI increase cloud lifetime, and thus cloudiness, by reducing droplet size and narrowing the droplet spectrum. Therefore, it is clear that the radiation and energy budget of the areas affected by the presence of dust, e.g., transport, can be altered directly and/or

indirectly. Hence, it is obvious that aerosols, and especially dust, which is the most abundant aerosol on a planetary scale, play a significant role in weather and climate patterns.

Although dust aerosols have been extensively investigated during the last decades, they contribute to one of the major uncertainties in climate model predictions [3]. Thus, there is need for improving scientific knowledge about dust transport, especially over areas like MB, which is close to the Sahara, Middle East, and Arabian deserts, and frequently undergoes dust transport, resulting in dust aerosol episodes (DAEs). In the present study, a satellite algorithm utilizing key aerosol optical properties is used in order to identify Dust Aerosol Episode Days (DAEDs), namely days characterized by the strong presence of dust, over the broader MB. The algorithm input data are spectral Aerosol Optical Depth (AOD) from the latest (Collection 6.1) MODIS-Aqua aerosol product (MYD08\_D3) and Aerosol Index (AI) from the latest version (OMAERUV) of OMI-Aura dataset. All input data are taken on a level 3 processing level, available on a daily and  $1^\circ \times 1^\circ$  pixel level basis. The algorithm operating at this spatial temporal resolution identifies dust aerosol episodes on a pixel level by applying specific threshold values to the utilized aerosol optical properties. When at least 30 dust episodic pixels are identified on a specific day, then this day is characterized as DAED. The algorithm operated for every day of the study period, spanning the years 2005 to 2019. The identified DAEDs are examined on a seasonal, annual as well as interannual basis.

## 2. Data and Methodology

### 2.1. MODIS and OMI Satellite Data

Data of AOD are taken from the MODIS-Aqua Collection 6.1 dataset. Collection 6.1 (C6.1) is the latest and improved, upon ground-based sun-photometer data collection, MODIS collection compared to the previous basic collection (C5) [4,5], but also to the C6 collection [6,7]. The utilized MODIS data provide spectral AOD information at three different wavelengths (470 nm, 550 nm and 660 nm) over land and at seven wavelengths (470 nm, 550 nm, 650 nm, 860 nm, 1240 nm, 1630 nm and 2130 nm) over water (ocean). In the present study, the level 3 MODIS Collection 6.1 aerosol product (MYD08\_D3) is used for the identification of dust in the atmosphere as well as for the computation of the Ångström Exponent (AE). Aerosol Index (AI) data are taken from the Ozone Monitoring Instrument (OMI) database. The OMI aerosol product provides data of AI, AOD and the Single Scattering Albedo (SSA), which have been evaluated against AERONET observations. Here, the level 3 product of the latest OMI edition (OMAERUV) is used. All input data (MODIS and OMI) are available on a daily and on a  $1^\circ \times 1^\circ$  longitude-latitude resolution. The selected study period spans the 15-year period from 1st January 2005 through to 31st December 2019, being constrained by the simultaneous availability of both MODIS and OMI data.

### 2.2. Methodology

The operation of the satellite algorithm utilized in the present study is based on MODIS AOD and OMI AI data and achieves the identification of Dust Aerosol Episodes (DAEs) over the broader MB on a daily and  $1^\circ \times 1^\circ$  pixel level basis. In the first step of the algorithm operation, a thresholding technique is applied in order to determine the presence of dust. Specifically, whenever AE is lower than or equal to 0.4 ( $AE \leq 0.4$ ), and AI is greater than or equal to 1 ( $AI \geq 1$ ), dust is considered the dominant aerosol in the atmospheric column. Dust having been identified, high aerosol loads are required in order to characterize a dusty pixel as an episodic one. The identified dust episodes are discriminated in two types, according to their intensity, in terms of aerosol load, i.e., AOD. When AOD is greater than or equal to its climatological mean value ( $AOD_{mean}$ ) plus two standard deviations (STDV), but lower than  $AOD_{mean}$  plus four STDVs, then the dust episode is characterized as strong. Otherwise, if AOD exceeds the  $AOD_{mean}$  plus four STDVs, then the episode is characterized as extreme. If at least 30 episodic pixels (strong or extreme) are determined on a specific day, this day is considered as a Dust Aerosol Episode Day

(DAED). For every DAED, the algorithm produces the spatial distribution of dust episodic pixels and the corresponding AOD. The algorithm's flowchart is depicted in Figure 1.

Following the algorithm runs for the entire study period (2005–2019), a climatological investigation of DAEDs is conducted, reproducing the mean seasonal and annual distributions as well as the interannual variability and trends of DAEDs' frequency, extent and intensity.

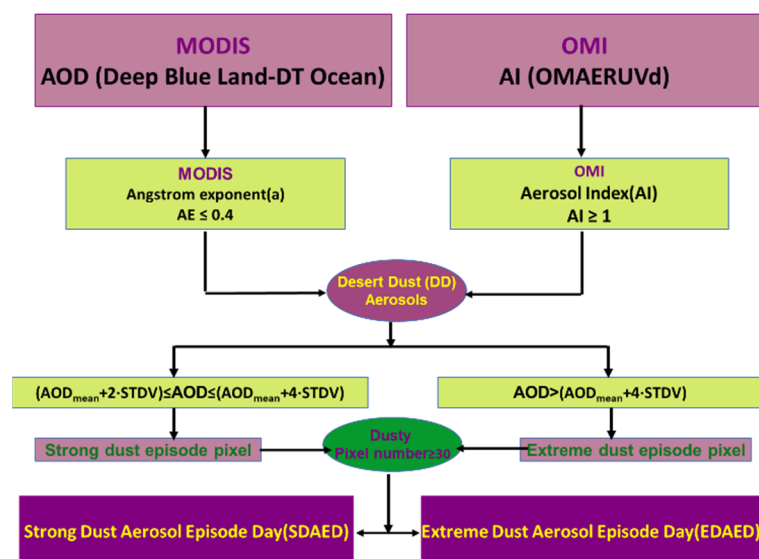


**Figure 1.** The satellite-based algorithm and the methodology applied for the identification of dust aerosols (DA).

### 3. Results and Discussion

#### 3.1. Seasonal Results

According to the algorithm results, 166 DAEDs took place in the MB from 2005 to 2019 (Table 1). In total, most of them occurred in the spring (46.9%) and summer (37.9%) periods, while only 9 out of 166 (5.4%) occurred in autumn. It should be noted that actually all of the autumn episodes were observed in September and October and none in November. Respectively, winter DAEDs refer only to January and February. These results are in line with previous studies [8,9], regarding the seasonality of dust episodes. However, the annual number of the identified DAEDs (11.1 DAEDs/year) is lower than the one (19.6 DAEDs/year) reported by [10], who applied a previous version of the satellite algorithm on a shorter study period, spanning from 2000 to 2007. This is mainly attributed to the use in the present study of a stricter AE threshold ( $AE \leq 0.4$ ) than in [10] ( $AE \leq 0.7$ ). Most (70%) of the identified DAEDs (116 out of 166, Table 1) are characterized as strong ones. The seasonality of strong DAEDs is similar that of all DAEDs, with a maximum frequency of occurrence in spring and summer. On the other hand, the extreme DAEDs have a different seasonal variability, being most frequent in the spring (52%) and winter (22%) periods.

**Table 1.** An overview of the average frequency of occurrence of dust aerosol episode days (DAEDs) that took place over the broader MB during the period 2005–2019.

| Number of DAEDs/Year<br>(Percentage) | WINTER    | SPRING     | SUMMER     | AUTUMN   | YEAR |
|--------------------------------------|-----------|------------|------------|----------|------|
| All (strong+extreme) episodes        | 16 (9.6%) | 78 (47%)   | 63 (38%)   | 9 (5.4%) | 166  |
| Strong episodes                      | 5 (4.3%)  | 52 (44.8%) | 54 (46.6%) | 5 (4.3%) | 116  |
| Extreme episodes                     | 11 (22%)  | 26 (52%)   | 9 (18%)    | 4 (8%)   | 50   |

### 3.2. Inter-Annual Variability and Trends

In Figure 2, the interannual variability and trends of DAEDs' properties, namely their frequency of occurrence, spatial extent and intensity, are displayed. Results are separately given for strong (first row) and extreme (second row) DAEDs. In general, the frequency of occurrence (first column) and the spatial extent (second column), which is here expressed in terms of the cumulative number of dusty pixels, exhibit a similar interannual variability for either strong or extreme episodes. For example, 2005, 2008 and 2018 are found to be very active years, with maximum frequencies of occurrence of DAEDs and number of dusty pixels, for both strong and extreme episodes. According to the algorithm results, no statistically significant trends are observed for strong DAEDs. On the other hand, it is found that the spatial extent and the intensity of extreme DAEDs (i.e., dust optical depth (DOD)) slightly decreased from 2005 to 2019. A similar decrease of DOD in the MB was also noted by [11], who used MODIS data from 2002 to 2017.

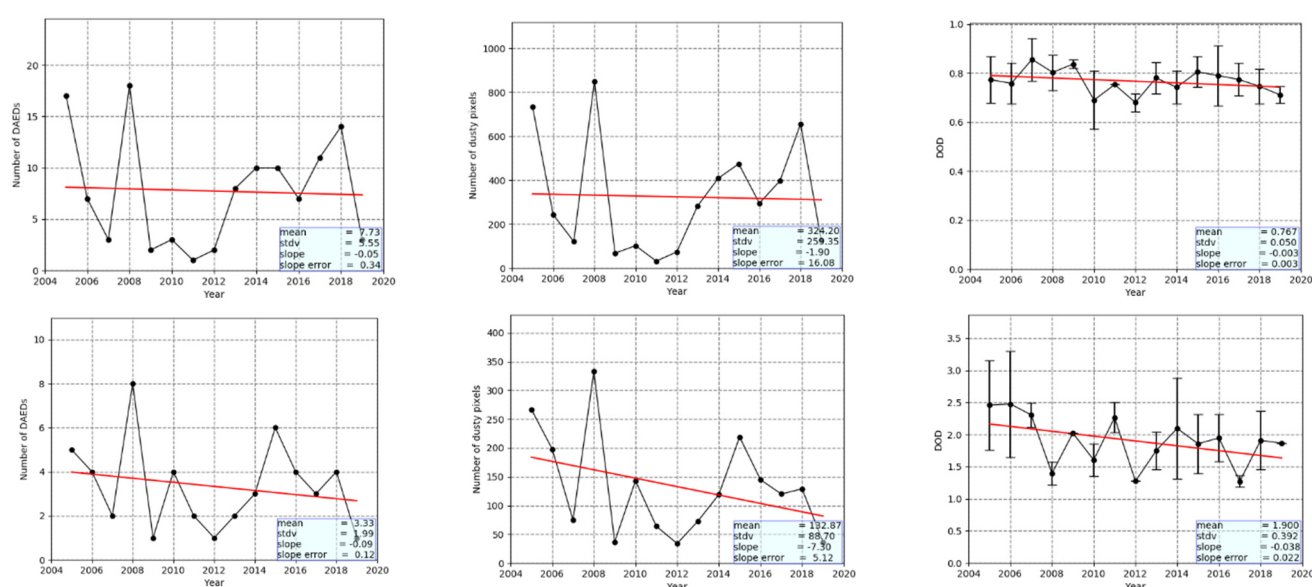


**Figure 2.** Inter-annual variation of: the total annual number of dust aerosol episode days (DAEDs) (left column), the annual total number of pixels undergoing dust aerosol episodes (middle column) and the mean annual dust optical depth (DOD) (right column). Results are averaged over the period 2005–2019, and they are given for strong dust episodes (first row) and extreme dust episodes (second row). The red line corresponds to the linear regression. The error bars in the right column results represent the temporal standard deviation associated with the mean annual DOD for each year of the study period (2005–2019).

### 3.3. Geographical Distributions

The total number of strong and extreme DAEDs that took place on a pixel level basis over the broader MB during the 15-study period (2005–2019) is given in Figure 3 (first row). Strong DAEDs are mainly observed over the western part of the study area, and especially over Algeria and Tunisia, where the frequency of occurrence is as high as 20–32 DAEDs per pixel (orange and reddish colors). Relatively high frequencies (up to 12 DAEDs/pixel) are also observed in the easternmost part of the area, i.e., over Syria. On the other hand, extreme dust episodes are more frequent over the central, and less over the eastern, parts of the Mediterranean, with maximum frequencies (up to 11 DAEDs/pixel) along the Tunisian coasts. In the second row of Figure 3, the geographical distribution of the annual mean DOD of DAEDs is displayed. It should be noted that the averaging of DOD was done taking into account only the episodic pixels/days and not all. The maximum DODs for strong DAEDs (up to 1.7) are observed along the coasts of Libya and Egypt, while the minimum ones (less than 0.4) over Italy and the western Balkans. On the other hand, the maximum DODs for extreme DAEDs (up to 4.9) are observed over the

central and eastern Mediterranean Sea. It is noted that the high DOD values over the Black Sea correspond to a single episode (see the top right map of the same figure). The geographical patterns of both frequency and intensity (DOD values are quite similar to those found in [9], who used a previous MODIS collection (C5) for the period 2000–2007, but here they also cover North Africa, thanks to the use of the Deep Blue algorithm in the MODIS C6.1 collection.

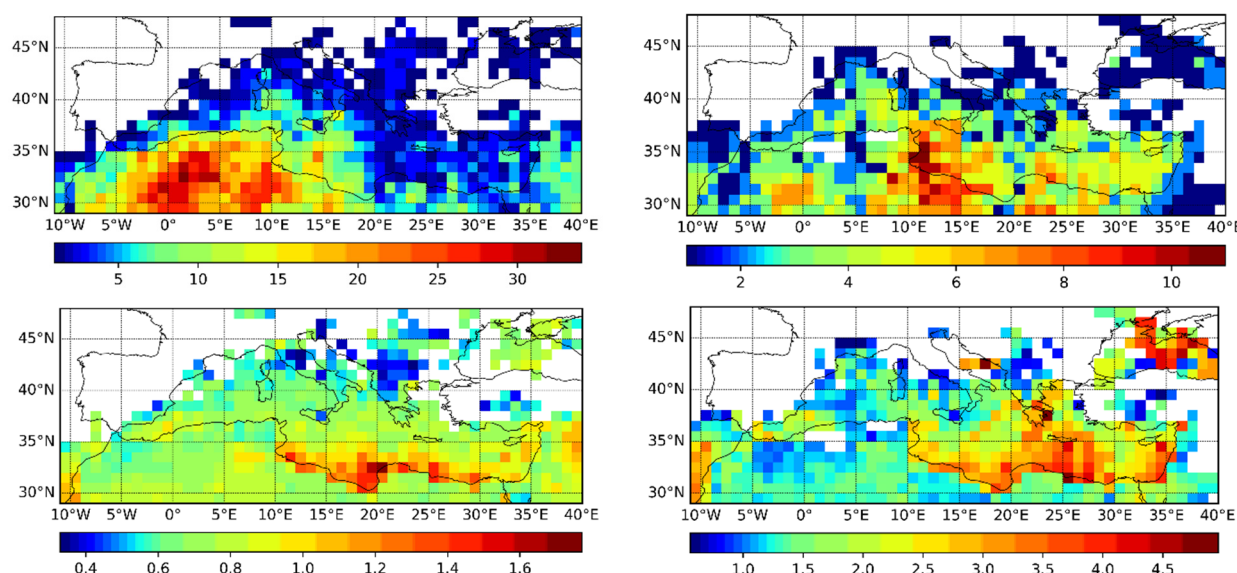


**Figure 3.** Spatial distribution of the total number of DAEDs (first row) and the corresponding mean annual DOD (second row). Results are given for strong (left column) and extreme (right column) DAEDs and refer to the 15-year period 2005–2019. White shaded pixels in the maps correspond to areas where no DAEDs at all have been identified during the study period.

#### 4. Conclusions

In the present study, dust aerosol episodes over the broader MB were identified on a  $1^\circ \times 1^\circ$  pixel level and on a 15-year study period (2005–2019) with an algorithm using contemporary MODIS and OMI satellite data. According to the algorithm results, 166 DAEDs (116 strong and 50 extreme) took place in the MB from 2005 to 2019. Most of them (84.8%) occurred in spring and summer, and the remaining 15.2% in autumn and winter, specifically during September, October, January and February, while no episodes at all were identified in November and December. Regarding the interannual variability of DAEDs, in general, no significant trends were found for strong episodes. In contrast, the spatial extent as well as the intensity of extreme DAEDs were found to have decreased during the period 2005–2019. The obtained geographical distributions indicate that strong DAEDs are more frequent in the western parts of the MB, while the extreme episodes are more widespread over the central and eastern parts of MB. High DOD values (up to 1.7 for strong and 4.9 for extreme episodes) were noted along the coasts of Libya and Egypt for both strong and extreme dust episodes. However, high DOD values of extreme episodes are more widespread, covering a big part of the eastern MB, including Greece (and especially its southern parts, namely Crete), the Ionian Sea, the Libyan Sea and the Syrian coasts.

**Author Contributions:** Conceptualization, N.H. and A.G.; methodology, N.H. and A.G.; software, N.H., A.G. and M.G.; formal analysis, M.G.; investigation, N.H. and M.G.; resources, N.H., M.G. and A.G.; data curation, N.H. and M.G.; writing—original draft preparation, M.G.; writing—review and editing, N.H., A.G., N.M. and M.G.; visualization, M.G.; supervision, N.H.; project administration, N.H.; funding acquisition, N.H. and N.M. All authors have read and agreed to the published version of the manuscript.

**Institutional Review Board Statement:** Not applicable.

**Informed Consent Statement:** Not applicable.

**Data Availability Statement:** Publicly available datasets were analyzed in this study. This data can be found here: <https://ladsweb.modaps.eosdis.nasa.gov/search/> (accessed on 31 March 2021).

**Acknowledgments:** We acknowledge the support of the project “PANhellenic infrastructure for Atmospheric Composition and climate change” (MIS 5021516), which is implemented under the Action “Reinforcement of the Research and Innovation Infrastructure”, funded by the Operational Programme “Competitiveness, Entrepreneurship and Innovation” (NSRF 2014–2020) and co-financed by Greece and the European Union (European Regional Development Fund).

## References

1. Twomey, S. Influence of pollution on shortwave albedo of clouds. *J. Atmos. Sci.* **1977**, *34*, 1149–1152, doi:10.1175/1520-0469(1977)034<1149:TIOPTO>2.0.CO;2.
2. Albrecht, B.A. Aerosols, cloud microphysics, and fractional cloudiness. *Science* **1989**, *245*, 1227–1230, doi:10.1126/science.245.4923.1227.
3. IPCC. *Climate Change 2013: The Physical Science Basis. Contribution of Working Group I to the Fifth Assessment Report of the Intergovernmental Panel on Climate Change*; Stocker, T.F., Qin, D., Plattner, G.-K., Tignor, M., Allen, S.K., Boschung, J., Nauels, A., Xia, Y., Bex, V., Midgley, P.M., Eds.; Cambridge University Press: Cambridge, UK; New York, NY, USA, 2013; 1535p, doi:10.1017/CBO9781107415324.
4. Levy, R.C.; Mattoo, S.; Munchak, L.A.; Remer, L.A.; Sayer, A.M.; Patadia, F.; Hsu, N.C. The Collection 6 MODIS aerosol products over land and ocean. *Atmos. Meas. Tech.* **2013**, *6*, 112989–113034.
5. Sayer, A.M.; Munchak, L.A.; Hsu, N.C.; Levy, R.C.; Bettenhausen, C.; Jeong, M.J. MODIS Collection 6 aerosol products: Comparison between Aqua’s e-Deep Blue, Dark Target, and “merged” data sets, and usage recommendations. *J. Geophys. Res. Atmos.* **2014**, *119*, 2413965–2413989.
6. Mattoo, S. Aerosol Dark Target (10km & 3km) Collection 6.1 Changes. 2017. Available online: [https://modis-atmosphere.gsfc.nasa.gov/sites/default/files/ModAtmo/C061\\_Aerosol\\_Dark\\_Target\\_v2.pdf](https://modis-atmosphere.gsfc.nasa.gov/sites/default/files/ModAtmo/C061_Aerosol_Dark_Target_v2.pdf) (accessed on 31 March 2021).
7. Hsu, N.C. Changes to MODIS Deep Blue Aerosol Products between Collection 6 and Collection 6.1. 2017. Available online: [https://atmosphere-imager.gsfc.nasa.gov/sites/default/files/ModAtmo/modis\\_deep\\_blue\\_c61\\_changes2.pdf](https://atmosphere-imager.gsfc.nasa.gov/sites/default/files/ModAtmo/modis_deep_blue_c61_changes2.pdf) (accessed on 31 March 2021).
8. Antoine, D.; Nobileau, D. Recent increase of Saharan dust transport over the Mediterranean Sea, as revealed from ocean color satellite (SeaWiFS) observations. *J. Geophys. Res.* **2016**, *111*, D12214, doi:10.1029/2005JD006795.
9. Gkikas, A.; Hatzianastassiou, N.; Mihalopoulos, N.; Katsoulis, V.; Kazadzis, S.; Pey, J.; Querol, X.; Torres, O. The regime of intense desert dust episodes in the Mediterranean based on contemporary satellite observations and ground measurements. *Atmos. Chem. Phys.* **2013**, *13*, 12135–12154, doi:10.5194/acp-13-12135-2013.
10. Gkikas, A.; Houssos, E.E.; Lolis, C.J.; Bartzokas, A.; Mihalopoulos, N.; Hatzianastassiou, N. Atmospheric circulation evolution related to desert-dust episodes over the Mediterranean. *Q. J. R. Meteorol. Soc.* **2015**, *141*, 1634–1645.
11. Yu, H.; Yang, Y.; Wang, H.; Tan, Q.; Chin, M.; Levy, R.C.; Remer, L.A.; Smith, S.J.; Yuan, T.; Shi, Y. Interannual variability and trends of combustion aerosol and dust in major continental outflows revealed by MODIS retrievals and CAM5 simulations during 2003–2017. *Atmos. Chem. Phys.* **2020**, *20*, 139–161, doi:10.5194/acp-20-139-2020.